Random antiferromagnetic quantum spin chains: Exact results from scaling of rare regions

Ferenc Iglói
Research Institute for Solid State Physics and Optics, P.O. Box 49, H-1525 Budapest, Hungary
and Institute for Theoretical Physics, Szeged University, H-6720 Szeged, Hungary

Róbert Juhász
Institute for Theoretical Physics, Szeged University, H-6720 Szeged, Hungary
and Research Institute for Solid State Physics and Optics, P.O. Box 49, H-1525 Budapest, Hungary

Heiko Rieger
Theoretische Physik, Universität des Saarlandes, D-66041 Saarbrücken, Germany
(Received 25 June 1999; revised manuscript received 11 November 1999)

We study *XY* and dimerized *XX* spin-1/2 chains with random exchange couplings by analytical and numerical methods and scaling considerations. We extend previous investigations to dynamical properties, to surface quantities, and operator profiles, and give a detailed analysis of the Griffiths phase. We present a phenomenological scaling theory of average quantities based on the scaling properties of rare regions, in which the distribution of the couplings follows a surviving random-walk character. Using this theory we have obtained the complete set of critical decay exponents of the random *XY* and *XX* models, both in the volume and at the surface. The scaling results are confirmed by numerical calculations based on a mapping to free fermions, which then lead to an exact correspondence with directed walks. The numerically calculated critical operator profiles on large finite systems ($L \leqslant 512$) are found to follow conformal predictions with the decay exponents of the phenomenological scaling theory. Dynamical correlations in the critical state are in average logarithmically slow and their distribution shows multiscaling character. In the Griffiths phase, which is an extended part of the off-critical region, average autocorrelations have a power-law form with a nonuniversal decay exponent, which is analytically calculated. We note on extensions of our work to the random antiferromagnetic *XXZ* chain and to higher dimensions.

I. INTRODUCTION

Quantum spin chains exhibit many interesting physical properties at low temperatures which are related to the behavior of their ground state and low-lying excitations. In this context one should mention quasi-long-range order (QLRO), topological order, and quantum phase transitions, which have purely quantum-mechanical origin. Considering isotropic antiferromagnetic chains for integer spins there is a gap, whereas half integer spin chains are gapless.[1] However, alternating couplings in spin-1/2 chains yield a dimerized ground state that has physical properties similar to the spin-1 chain: there is a finite gap, spatial correlations decay exponentially, and there is string topological order.

Randomness may have a profound effect on the physical properties of quantum spin chains, as demonstrated by recent analytical and numerical studies.[2] As an interplay of randomness and quantum fluctuations there are interesting exotic phases in disordered quantum spin chains, which are not present in classical random or pure quantum systems. It has been noticed that pure gapless systems are generally unstable against weak randomness,[3,4] whereas for gapped systems a finite amount of disorder is necessary to destroy the gap[5–7] (but see also Ref. 8).

Among the theoretical methods developed for disordered quantum spin chains one very powerful procedure is the renormalization group (RG) approach introduced by Dasgupta and Ma.[3] This RG method, which is expected to be asymptotically exact at large scales, i.e., close to critical points, has been applied for a number of random quantum systems. The fixed point distribution of the RG transformation has been obtained analytically for some random quantum spin chains, among others for the transverse Ising spin chain,[9] the spin-1/2 Heisenberg, and related spin chains with random antiferromagnetic couplings.[4] On the other hand, some other one-dimensional problems ($S=1/2$ Heisenberg chain with mixed ferromagnetic and antiferromagnetic couplings,[10,11] $S=1$ antiferromagnetic chain with and without biquadratic exchange,[5–7] etc.), as well as higher dimensional random quantum systems,[12] have been studied by numerical implementation of the RG procedure. Comparing the RG results with those obtained by direct numerical evaluation of the singular quantities[13–16] and by other exact[17,15] and numerical methods one has obtained a good agreement in the vicinity of the critical point.

There are, however, other interesting singular quantities, which are not accessible by the RG method. We mention, among others, the dynamical correlations[18] and the behavior of the system far away from the critical point in the Griffiths phase,[19] which denotes an extended region of the parameter space around the critical point. In the Griffiths phase the system is gapless, and thus dynamical correlations decay with a power law, although there is long-range order with exponentially decaying spatial correlations. For the random quantum Ising chain dynamical correlations, both at the critical point and in the Griffiths phase, have been exactly

determined[20–22] using a mapping to the Sinai model,[23] i.e., random walk in a random environment.

In this paper we are going to study the $S=1/2$ disordered *XX* and *XY* spin chains by analytical and numerical methods and by phenomenological scaling theory. The RG treatment of the problem by Fisher[4] predicts that the antiferromagnetic random *XX* fixed point controls the critical behavior of the antiferromagnetic Heisenberg (*XXX*) model, too. Furthermore, for random isotropic chains the RG approach predicts QLRO, and thus the average spatial correlations of different components of the spin decays with a power law. In this so-called random singlet (RS) phase all spins are paired and form singlets, but the distance between the two spins in a singlet pair can be arbitrarily large. Then these weakly coupled singlets dominate the average correlation function. Therefore all components of the correlation function are predicted to decay with the same exponent.

By the introduction of either anisotropy or dimerization the system becomes noncritical, but, randomness will drive the system into the Griffiths phase, which is still gapless. As shown by an RG analysis,[5] applicable in the vicinity of the RS fixed point, the Griffiths phase is characterized by the dynamical exponent *z*, defined by the asymptotic relation between relevant time (t_r) and length scales (ξ) as

$$t_r \sim \xi^z. \tag{1.1}$$

The dynamical exponent is predicted to be a continuous function of the quantum control parameter (anisotropy or dimerization) and the singular behavior of different physical quantities (specific heat, susceptibility, etc.) are all expected to be related to the value of the dynamical exponent.

The RG predictions by Fisher[4] and others[5] have been scrutinized by numerical studies,[24–26] especially in the RS phase of isotropic chains. Some crossover functions of correlations have also been studied in the Griffiths phase. In the RS phase some numerical results are controversial: in earlier studies[25] a different scenario from the RG picture is proposed (in particular with respect to the transverse correlation function), but later investigations on larger finite systems have found satisfactory agreement with the RG predictions,[26] although the finite-size effects were still very strong.

In the present paper we extend previous work in several directions. Here we consider open chains and study both bulk and surface quantities, as well as end-to-end correlations. We develop a phenomenological theory which is based on the scaling properties of rare events and determine the complete set of critical decay exponents.[27] We calculate numerically (off-diagonal) spin-operator profiles, whose scaling properties are related to (bulk and surface) decay exponents[28] and compare the profiles with predictions of conformal invariance. Another feature of our work is the study of dynamical correlations, both at the critical point and in the Griffiths phase. Finally, we perform a detailed analytical and numerical study of the Griffiths phase and calculate, among others, the exact value of the dynamical exponent *z* in Eq. (1.1).

The structure of the paper is the following. The model and its free-fermion representation are presented in Sec. II. A phenomenological theory based on the scaling behavior of rare events is developed in Sec. III. Results in the critical state, where there is quasi-long-range order in the chains is presented in Sec. IV, whereas the Griffiths phase is studied in Sec. V. We discuss the extensions of our results to random antiferromagnetic *XXZ* chains and to higher dimensions in the final section, whereas some technical calculations are presented in the appendixes.

II. THE MODEL AND ITS FREE-FERMION REPRESENTATION

A. *XY* and *XX* models

We consider an open *XY* chain (i.e., with free boundary conditions) with *L* sites described by the Hamiltonian

$$H=\sum_{l=1}^{L-1} (J_l^x S_l^x S_{l+1}^x + J_l^y S_l^y S_{l+1}^y), \tag{2.1}$$

where the S_l^μ ($\mu=x,y$) are spin-1/2 operators and the couplings ($J_l^\mu>0$) are independent random variables with distributions $\pi^\mu(J^\mu)$. The quantum control parameter is the average anisotropy defined as

$$\delta_a=\frac{[\ln J^x]_{\rm av}-[\ln J^y]_{\rm av}}{{\rm var}[\ln J^x]+{\rm var}[\ln J^y]}, \tag{2.2}$$

where var(x) is the variance of random variable x and $[\cdots]_{\rm av}$ denotes the average over quenched disorder. For $\delta_a>0$ (<0) there is long-range order in the x (y) direction, i.e., $\lim_{r\to\infty}[C^\mu(r)]_{\rm av}\neq 0$, where

$$[C^\mu(r)]_{\rm av}=[\langle 0|S_l^\mu S_{l+r}^\mu|0\rangle]_{\rm av}, \tag{2.3}$$

and for $\delta_a=0$ the system is in a critical state with quasi-long-range order, where correlations decay algebraically, i.e.,

$$[C^\mu(r)]_{\rm av}\sim r^{-\eta^\mu}. \tag{2.4}$$

In the *XX* model, where the *x* and *y* couplings are correlated as $J_l^x=J_l^y=J_l$, we introduce alternation such that even (e) and odd (o) couplings, connecting the site $2i,2i+1$ and $2i-1,2i$, respectively, are taken from distributions $\rho^e(J_e)$ and $\rho^o(J_o)$, respectively. For the *XX* model the quantum control parameter is the average dimerization defined as

$$\delta_d=\frac{[\ln J_o]_{\rm av}-[\ln J_e]_{\rm av}}{{\rm var}[\ln J_o]+{\rm var}[\ln J_e]}. \tag{2.5}$$

The RS phase is at $\delta_d=0$, whereas $\delta_d\neq 0$ corresponds to the random dimer (RD) phase. Throughout the paper we use two types of random distributions, both for the *XY* and *XX* models. For the *XY* model with the binary distribution the J^x couplings can take two values $\lambda>1$ and $1/\lambda$ with probability p and $q=1-p$, respectively, while the couplings J^y are constant:

$$\pi^x(J^x)=p\,\delta(J^x-\lambda)+q\,\delta(J^x-\lambda^{-1}),$$

$$\pi^y(J^y)=\delta(J^y-J_0^y). \tag{2.6}$$

At the critical point $(p-q)\ln\lambda=\ln J_0^y$. The uniform distribution is defined via

$$\pi^x(J^x)=\begin{cases}1, & \text{for } 0<J^x<1\\ 0, & \text{otherwise,}\end{cases}$$

$$\pi^y(J^y)=\begin{cases}(J_0^y)^{-1}, & \text{for } 0<J^y<J_0^y\\ 0, & \text{otherwise}\end{cases} \tag{2.7}$$

and the critical point is at $J_0^y=1$.

For the *XX* model the corresponding distributions $\rho^e(J^e)$ and $\rho^o(J^o)$ follows from the correspondences

$$J^x\to J^e,\quad J^y\to J^o,\quad \pi^x(J^x)\to\rho^e(J^e),\quad \pi^y(J^y)\to\rho^o(J^o). \tag{2.8}$$

Note that the critical points of the two models ($\delta_a=0$ and $\delta_d=0$, respectively) are not equivalent due to the different disorder correlations.

B. *XY* chain and the directed walk model

Using the Jordan-Wigner transformation, the *XY* model Hamiltonian in Eq. (2.1) can be rewritten as a quadratic form in fermion operators. It is then diagonalized through a canonical transformation which gives

$$S_l^xS_{l+1}^x=\frac{1}{4}B_lA_{l+1},\quad S_l^yS_{l+1}^y=-\frac{1}{4}A_lB_{l+1}, \tag{2.9}$$

with

$$A_i=\sum_{q=1}^{L}\Phi_q(i)(\eta_q^+ +\eta_q),$$
$$B_i=\sum_{q=1}^{L}\Psi_q(i)(\eta_q^+ -\eta_q), \tag{2.10}$$

in terms of the fermion creation (η_q^+) and annihilation (η_q) operators. Then the Hamiltonian assumes the diagonal form

$$H=\sum_{q=1}^{L}\epsilon_q\left(\eta_q^+\eta_q-\frac{1}{2}\right), \tag{2.11}$$

where the ordering of the fermionic states is given with increasing energy ϵ_q. The fermion excitations are nonnegative and satisfy the set of equations

$$\epsilon_q\Psi_q(l)=J_{l-1}^y\Phi_q(l-1)+J_l^x\Phi_q(l+1),$$
$$\epsilon_q\Phi_q(l)=J_{l-1}^x\Psi_q(l-1)+J_l^y\Psi_q(l+1) \tag{2.12}$$

with the boundary conditions $J_L^x=J_L^y=0$. The vectors Φ_q's and Ψ_q's which are related to the coefficients of the canonical transformation are normalized. They enter into the expressions of correlation functions and thermodynamic quantities.

Usually one proceeds[29] by eliminating either Ψ_q or Φ_q in Eqs. (2.12) and the excitations are deduced from the solution of quadratic equations. This last step can be avoided by introducing a $2L$-dimensional vector V_q with components

$$V_q(4l-3)=\Phi_q(2l-1),\qquad V_q(4l-2)=\Psi_q(2l-1),$$
$$V_q(4l-1)=\Psi_q(2l),\qquad V_q(4l)=\Phi_q(2l) \tag{2.13}$$

and noticing that the relations in Eqs. (2.12) then correspond to the eigenvalue problem of the matrix

$$T=\begin{pmatrix}
0 & 0 & J_1^y & & & & & & & \\
0 & 0 & 0 & J_1^x & & & & & & \\
J_1^y & 0 & 0 & 0 & J_2^x & & & & & \\
 & J_1^x & 0 & 0 & 0 & J_2^y & & & & \\
 & & J_2^x & 0 & 0 & 0 & J_3^y & & & \\
 & & & J_2^y & 0 & 0 & 0 & \ddots & & \\
 & & & & \ddots & \ddots & \ddots & \ddots & J_{L-1}^y & \\
 & & & & & J_{L-2}^y & 0 & 0 & 0 & J_{L-1}^x \\
 & & & & & & J_{L-1}^y & 0 & 0 & 0 \\
 & & & & & & & J_{L-1}^x & 0 & 0
\end{pmatrix}. \tag{2.14}$$

The matrix T can be interpreted as the transfer matrix (TM) of a directed walk (DW) problem on four interpenetrating, diagonally layered square lattices. Each walker makes steps with weights J_l^x and J_l^y between next-neighbor sites on one of the four square lattices and the walk is directed in the diagonal direction (see Fig. 1).

According to Eqs. (2.12), changing Φ_q into $-\Phi_q$ in V_q, the eigenvector corresponding to $-\epsilon_q$ is obtained. Thus all information about the DW and the *XY* model is contained in that part of the spectrum with $\epsilon_q\geqslant 0$. Later on we shall consider this sector. We note that similar correspondence has been established earlier between the DW and the transverse-field Ising model (TIM).[30]

The eigenvalues of T in Eq. (2.14) consist of two classes. For $q=2i-1$, $i=1,2,\ldots,L$ the odd components of the eigenvectors are zero, i.e., $V_{2i-1}(2j)=0$, $j=1,2,\ldots,L$, whereas for the other class with $q=2i$ the even components are zero, $V_{2i}(2j-1)=0$. Consequently, T can be expressed as a direct product $T=T_\sigma\otimes T_\tau$, where the trigonal matrices T_σ, T_τ of size $L\times L$ represent transfer matrices of directed

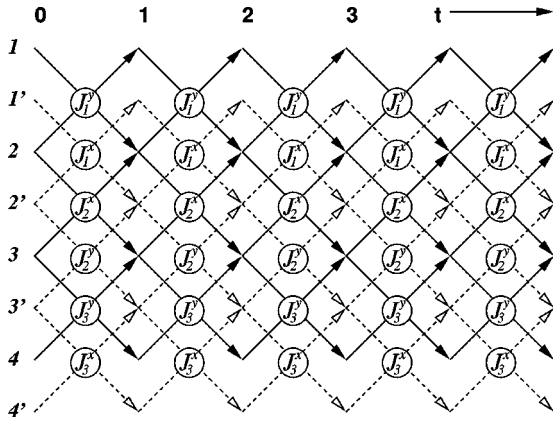

FIG. 1. Sketch of the directed walk problem corresponding to the transfer matrix given in Eq. (2.14). Note that one has two independent walks in the **t** direction of the diagonally layered square lattice, corresponding to the independent subspaces for the eigenvalue problem (see text). The coupling strength $J_i^{x,y}$ are the transition rates for the random walker from one site in row i to those in row $i\pm1$.

walks. As a result one has to diagonalize these two matrices of size $L\times L$. Thus for chains with even number of sites, $L=2N$, the two classes of eigenvectors are given in terms of the variables Φ and Ψ via

$$\epsilon_{2k-1}: \quad \Phi_{2k-1}(2j)=\Psi_{2k-1}(2j-1)=0,$$
$$\epsilon_{2k}: \quad \Phi_{2k}(2j-1)=\Psi_{2k}(2j)=0 \tag{2.15}$$

for $i,j=1,\ldots,N$. Furthermore we assume that the vectors $\mathbf{\Phi}_q$ and $\mathbf{\Psi}_q$ are normalized to 1 separately.

For the XX model the even and odd sectors are degenerate, $\epsilon_{2k-1}=\epsilon_{2k}$. Thus it is sufficient to diagonalize only one matrix. In this case one has the additional relations

$$\begin{aligned}\Phi_{2k-1}(2j-1)&=\Psi_{2k}(2j-1),\\ \Phi_{2k}(2j)\qquad&=\Psi_{2k-1}(2j).\end{aligned} \quad XX \text{ model} \tag{2.16}$$

The matrices T_σ and T_τ are in one-to-one correspondence with the eigenvalue problem of one-dimensional TIM's. This exact mapping for finite open chains is presented in Appendix A.

C. Local order parameters

Next we are going to study the long-range order in the ground state of the system. Having free boundary conditions, as in Eq. (2.1), the expectation value of the local spin operator $\langle 0|S_l^x|0\rangle$ (and $\langle 0|S_l^y|0\rangle$) is zero for finite chains. Then the scaling behavior of the spin operator can be obtained from the asymptotic behavior of the (imaginary) time-time correlation function:

$$G_l^x(\tau)=\langle 0|S_l^x(\tau)S_l^x(0)|0\rangle$$
$$=\sum_{\langle n|}|\langle n|S_l^x|0\rangle|^2\exp[-\tau(E_n-E_0)], \tag{2.17}$$

where $|0\rangle$ and $|n\rangle$ denote the ground state and the nth excited state of H in Eq. (2.1), with energies E_0 and E_n, respectively. In the phase with long-range order the first excited state is asymptotically degenerate with the ground state in the thermodynamic limit, thus the sum in Eq. (2.17) is dominated by the first term. In the large τ limit $\lim_{\tau\to\infty}G_l^x(\tau)=(m_l^x)^2$, thus the local order parameter is given by the off-diagonal matrix element

$$m_l^x=\langle 1|S_l^x|0\rangle. \tag{2.18}$$

In the free fermion representation S_l^x is expressed as[29]

$$S_l^x=\frac{1}{2}A_1B_1A_2B_2\cdots A_{l-1}B_{l-1}A_l. \tag{2.19}$$

Using $|1\rangle=\eta_1^+|0\rangle$, the matrix element in Eq. (2.18) is evaluated by Wick's theorem. Since for $i\neq j$ $\langle 0|A_iA_j|0\rangle=\langle 0|B_iB_j|0\rangle=0$ we obtain for the local order parameter

$$m_l^x=\frac{1}{2}\begin{vmatrix} H_1 & G_{11} & G_{12} & \ldots & G_{1l-1}\\ H_2 & G_{21} & G_{22} & \ldots & G_{2l-1}\\ \vdots & \vdots & \vdots & \ddots & \vdots\\ H_l & G_{l1} & G_{l2} & \ldots & G_{ll-1}\end{vmatrix}, \tag{2.20}$$

where

$$H_j=\langle 0|\,\eta_1A_j|0\rangle=\Phi_1(j),$$
$$G_{jk}=\langle 0|B_kA_j|0\rangle=-\sum_q\Psi_q(k)\Phi_q(j). \tag{2.21}$$

For surface spins the local order parameter is simply given by $m_1^x=\Phi_1(1)/2$, which can be evaluated in the thermodynamic limit $L\to\infty$ in the phase with long-range order, when $\epsilon_1=0$. Using the normalization condition $\Sigma_l|\Phi_1(l)|^2=1$, we obtain for the surface order parameter

$$m_1^x=\frac{1}{2}\left[1+\sum_{l=1}^{L/2-1}\prod_{j=1}^{l}\left(\frac{J_{2j-1}^y}{J_{2j}^x}\right)^2\right]^{-1/2} XY,$$
$$m_1^x=\frac{1}{2}\left[1+\sum_{l=1}^{L/2-1}\prod_{j=1}^{l}\left(\frac{J_{2j-1}}{J_{2j}}\right)^2\right]^{-1/2} XX. \tag{2.22}$$

We note that this formula is *exact* for finite chains if we use fixed spin boundary condition, $S_L^x=\pm1/2$, which amounts to have $J_{L-1}^y=0$. In the fermionic description the twofold degeneracy of the energy levels, corresponding to $S_L^x=1/2$ and $S_L^x=-1/2$, is manifested by a zero energy mode in Eq. (2.11) and from the corresponding eigenvector one obtains m_1^x in Eq. (2.22) for any finite chain.

For nonsurface spins the expression of the local order parameter in Eq. (2.20) can be simplified by using the relations in Eq. (2.15). Then, half of the elements of the determinant in Eq. (2.20) are zero, the nonzero elements being arranged in a checkerboard pattern, and m_l^x can be expressed as a product of two determinants of half size, which reads for $l=2j$ as

$$m^x_{2j}=\frac{1}{2}\begin{vmatrix} H_1 & G_{1,2} & G_{1,4} & \dots & G_{1,2j-2} \\ H_3 & G_{3,2} & G_{3,4} & \dots & G_{3,2j-2} \\ \vdots & \vdots & \vdots & \ddots & \vdots \\ H_{2j-1} & G_{2j-1,2} & G_{2j-1,4} & \dots & G_{2j-1,2j-2} \end{vmatrix}$$

$$\times\begin{vmatrix} G_{2,1} & G_{2,3} & \dots & G_{2,2j-1} \\ G_{4,1} & G_{4,3} & \dots & G_{4,2j-1} \\ \vdots & \vdots & \ddots & \vdots \\ G_{2j,1} & G_{2j,3} & \dots & G_{2j,2j-1} \end{vmatrix}. \tag{2.23}$$

The local order parameter m^y_l, related to the off-diagonal matrix element of the operator S^y_l can be obtained from Eqs. (2.20) and (2.22) by exchanging $J^x_l \leftrightarrow J^y_l$.

For the S^z_l operator the autocorrelation function $G^z_l(\tau)$ can be expressed in a similar way as $G^x_l(\tau)$ in Eq. (2.17) and its long time limit, $\lim_{\tau\to\infty} G^z_l(\tau)=(m^z_l)^2$, is given by the local order parameter

$$m^z_l=\langle\phi_z|S^z_l|0\rangle. \tag{2.24}$$

Here $|\phi_z\rangle$ denotes the lowest eigenstate of H in Eq. (2.1) having a nonvanishing matrix element of S^z_l with the ground state. In the free fermion representation S^z_l can be written as[29]

$$S^z_l=\tfrac{1}{2}A_lB_l \tag{2.25}$$

and the off-diagonal order parameter is given by

$$m^z_l=\tfrac{1}{2}\,|-\Phi_1(l)\Psi_2(l)+\Psi_1(l)\Phi_2(l)|. \tag{2.26}$$

For the XX model one can obtain simple expressions using the relations in Eqs. (2.16) as

$$m^z_{2i-1}=\tfrac{1}{2}[\Phi_1(2i-1)]^2,$$
$$m^z_{2i}=\tfrac{1}{2}[\Psi_1(2i)]^2. \qquad XX \text{ model} \tag{2.27}$$

D. Autocorrelations

Next we consider the dynamical correlations of the system as a function of the imaginary time τ. First, we note that the correlations between x components of the surface spins can be obtained directly from Eq. (2.17) as

$$G^x_1(\tau)=\frac{1}{4}\sum_q |\Phi_q(1)|^2\exp(-\tau\epsilon_q)$$
$$=\frac{1}{4}\sum_i^{L/2}|\Phi_{2i-1}(1)|^2\exp(-\tau\epsilon_{2i-1}), \tag{2.28}$$

where we have used the relations in Eq. (2.15).

For bulk spins the matrix element $\langle n|S^x_l|0\rangle$ in Eq. (2.17) is more complicated to evaluate. One has to go back to the first equation of Eq. (2.17) and considers the time evolution in the Heisenberg picture:

$$S^x_l(\tau)=\exp(\tau H)S^x_l\exp(-\tau H)$$
$$=\tfrac{1}{2}A_1(\tau)B_1(\tau)\cdots A_{l-1}(\tau)B_{l-1}(\tau)A_l(\tau). \tag{2.29}$$

The general time and position dependent correlation function

$$\langle S^x_l(\tau)S^x_{l+n}\rangle=\tfrac{1}{4}\langle A_1(\tau)B_1(\tau)\cdots A_l(\tau)A_1B_1\cdots A_{l+n}\rangle, \tag{2.30}$$

where the brackets $\langle\cdots\rangle$ either mean the ground-state expectation value at zero temperature or the thermal expectation value at nonvanishing temperature, can then be expanded using Wick's theorem into a sum over products of two-operator expectation values, which can be expressed in a compact form as a Pfaffian:

$$4\langle S^x_l(\tau)S^x_{l+n}\rangle=\begin{vmatrix} \langle A_1(\tau)B_1(\tau)\rangle & \langle A_1(\tau)A_2(\tau)\rangle & \langle A_1(\tau)B_2(\tau)\rangle & \cdots & \langle A_1(\tau)A_l(\tau)\rangle & \langle A_1(\tau)A_1\rangle & \cdots & \langle A_1(\tau)A_{l+n}\rangle \\ & \langle B_1(\tau)A_2(\tau)\rangle & \langle B_1(\tau)B_2(\tau)\rangle & \cdots & \langle B_1(\tau)A_l(\tau)\rangle & \langle B_1(\tau)A_1\rangle & \cdots & \langle B_1(\tau)A_{l+n}\rangle \\ & & \langle A_2(\tau)B_2(\tau)\rangle & \cdots & \langle A_2(\tau)A_l(\tau)\rangle & \langle A_2(\tau)A_1\rangle & \cdots & \langle A_2(\tau)A_{l+n}\rangle \\ & & & & \ddots & & \vdots & \\ & & & & & & & \langle B_{l+n-1}A_{l+n}\rangle \end{vmatrix}$$
$$=\pm[\det C_{ij}]^{1/2}. \tag{2.31}$$

In Eq. (2.31) C_{ij} is an antisymmetric matrix $C_{ij}=-C_{ji}$, with the elements of the Pfaffian (2.31) above the diagonal. At zero temperature the elements of the Pfaffian are the following:

$$\langle A_j(\tau)A_k\rangle=\sum_q \Phi_q(j)\Phi_q(k)\exp(-\tau\epsilon_q),$$

$$\langle A_j(\tau)B_k\rangle=\sum_q \Phi_q(j)\Psi_q(k)\exp(-\tau\epsilon_q),$$

$$\langle B_j(\tau)B_k\rangle=-\sum_q \Psi_q(j)\Psi_q(k)\exp(-\tau\epsilon_q),$$

$$\langle B_j(\tau)A_k\rangle=-\sum_q \Psi_q(j)\Phi_q(k)\exp(-\tau\epsilon_q), \quad (2.32)$$

whereas the equal-time contractions are given below Eq. (2.10). For the finite temperature contractions, see Ref. 31.

For longitudinal correlations the matrix elements of S_l^z in Eq. (2.25) is given in a simple form for any position l, therefore $G_l^z(\tau)$ can be obtained from the analogous expression to Eq. (2.17) as

$$G_l^z(\tau)=\frac{1}{4}\sum_q\sum_{p>q}|-\Psi_p(l)\Phi_q(l)+\Psi_q(l)\Phi_p(l)|^2 \times\exp[-\tau(\epsilon_q+\epsilon_p)]. \quad (2.33)$$

III. PHENOMENOLOGICAL THEORY FROM SCALING OF RARE EVENTS

In classical random ferromagnets where the critical behavior is controlled by a random fixed point the distribution of several physical quantities (order parameters, correlations, autocorrelations, etc.) is broad and as a consequence these quantities are not self-averaging: their average and most probable or typical values are different. In random quantum spin chains the critical properties are expected to be controlled by the infinite-randomness critical fixed point,[32] where the distributions are extremely (logarithmically) broad and as a consequence the average and typical behavior of these quantities are completely different. The average is dominated by realizations (the so called *rare events*), which have a very large contribution, but their fraction is vanishing in the thermodynamic limit. In this section we identify these rare events for the random *XY* (and *XX*) model and use their properties to develop a phenomenological theory. Our basic observations are related to exact relations about the surface order parameter and the energy of low-lying excitations.

A. Surface order parameter and the mapping to adsorbing random walks

The local order parameter at the boundary is given by the simple formula in Eq. (2.22) as a sum of products of the ratio of the couplings J_{2j-1}^y and J_{2j}^x. It is easy to see from Eq. (2.22) that in the thermodynamic limit the average surface order parameter is zero (nonzero), if the geometrical mean of the J_{2j}^x couplings is greater (smaller) than that of the J_{2j-1}^y couplings. From this the definition of the control parameters in Eqs. (2.2) and (2.5) follows.

Next we compute the average value of the surface order parameter for the extreme binary distribution,[33], i.e., the limit $\lambda\to 0$ in Eq. (2.6). For a random realization of the couplings the surface order parameter at the critical point ($p=q=1/2$) is zero, whenever a product of the form of $\Pi_{i=1}^{l}(J_i^x)^{-2}$, $l=1,2,\ldots,L$ is infinite, i.e., the number of λ couplings exceeds the number of λ^{-1} couplings in any of the $[1,l]$ intervals. Otherwise the surface order parameter has a finite value of $O(1)$. The distribution of the couplings J^x can be represented by one-dimensional random walks that start at zero and make the ith step upwards (for $J_{2i}^x=\lambda^{-1}$) or downwards (for $J_{2i}^x=\lambda$). The ratio of walks representing a sample with finite surface order parameter is given by the survival probability of the walk $P_{\rm surv}$, i.e., the probability of the walker to stay always above the starting point in $L/2$ steps which is given by $P_{\rm surv}(L/2)\sim L^{-1/2}$.

Next we consider the vicinity of the critical point, when the scaling behavior of the average surface order parameter can be obtained from the survival probabilities of biased random walks,[15] where the probability that the walker makes a step towards the adsorbing boundary q is different from that of a step off the boundary p. The control parameter of the walk, $\delta_w=p-q$, is analogous to the quantum control parameters δ_a and δ_d in Eqs. (2.2) and (2.5), respectively. Thus we have the basic correspondences between the average surface order parameter of the *XY* (and *XX*) model and the surviving probability of adsorbing random walks:

$$[m_1(\delta,L)]_{\rm av}\sim P_{\rm surv}(\delta_w,L/2), \qquad \delta\sim\delta_w. \quad (3.1)$$

We recall the asymptotic properties of the surviving probability of adsorbing random walks.[15] For unbiased walks,

$$P_{\rm surv}(\delta_w=0,L)\sim L^{-1/2}, \quad (3.2)$$

for walks with a drift away from the wall,

$$P_{\rm surv}(\delta_w>0,L\to\infty)\sim\delta_w, \quad (3.3)$$

and for walks with a drift towards the wall,

$$P_{\rm surv}(\delta_w<0,L)\sim\exp(-L/\xi_w), \qquad \xi_w\sim\delta_w^{-2}. \quad (3.4)$$

In this way we have identified the rare events for the surface order parameter, which are samples with a coupling distribution which have a surviving walk character. The scaling properties of the average surface order parameter and the correlation length immediately follow from Eqs. (3.2), (3.3), and (3.4) and will be evaluated in Sec. IV A.

B. Scaling of low-energy excitations

The rare events controlling the surface order parameter are also important for the low-energy excitations. Our results are obtained by using a simple relation for the smallest gap $\epsilon_1(l)$ of an open system of size l, i.e., with free boundary conditions, expecting that it goes to zero at least as $\sim 1/l$. With this condition one can neglect the right-hand side of the eigenvalue problem of $\mathbf{T}^2$ as $\mathbf{T}^2V_1=\epsilon_1^2V_1$, since terms at the left-hand side in a second-order difference equation are of $O(l^{-2})$. In this way one derives approximate expressions for the eigenfunctions Φ_1 and Ψ_1 and with these then one gets from the first equation of Eq. (2.12), i.e., with $l=1$,

$$\epsilon_1(l)\sim m_1^x m_{l-1}^x J_{l-1}^y\prod_{j=1}^{l/2-1}\frac{J_{2j-1}^y}{J_{2j}^x}. \quad (3.5)$$

Here m_1^x is defined in Eq. (2.22) and the surface order parameter at the other end of the chain, m_{l-1}^x, is given as in Eq. (2.22) replacing J_{2j-1}^y/J_{2j}^x by J_{l+1-2j}^y/J_{l-2j}^x. (For details of the derivation of a similar expression for the quantum Ising chain, see Ref. 34.)

Before using the relation in Eq. (3.5), we note that (surface) order and the presence of low-energy excitations are inherently related. These samples with an exponentially (in the system size) small gap have finite, $O(1)$, order parameters at both boundaries and the coupling distribution follows a surviving walk picture. Such type of coupling configuration represents a strongly coupled domain (SCD), which at the critical point extends over the size of the system L. In the off-critical situation, in the Griffiths phase the SCD's have a smaller extent, $l \ll L$, and they are localized both in the volume and near the surface of the system. The characteristic excitation energy of an SCD can be estimated from Eq. (3.5) as

$$\epsilon_1(l) \sim \prod_{j=1}^{l/2-1} \frac{J_{2j-1}^y}{J_{2j}^x} \sim \exp\left\{ -\frac{l_{\rm tr}}{2} \overline{\ln(J^y/J^x)} \right\}, \qquad (3.6)$$

where $l_{\rm tr}$ measures the size of transverse fluctuations of a surviving walk of length l and $\overline{\ln(J^x/J^y)}$ is an average ratio of the couplings, (it is $\overline{\ln(J^e/J^o)}$ for the XX model).

At the critical point ($\delta=0$), where $l \sim L$, the size of transverse fluctuations of the couplings in the SCD (Ref. 15) is $l_{\rm tr} \sim L^{1/2}$. Consequently we obtain from Eq. (3.6) for the scaling relation of the gap

$$\epsilon_1(\delta=0,L) \sim \exp(-\text{const} \cdot L^{1/2}). \qquad (3.7)$$

Then the appropriate scaling variable is $\ln \epsilon/\sqrt{L}$ and the distribution of the excitation energy is extremely (logarithmically) broad.

In the Griffiths phase the size of an SCD can be estimated along the lines of Ref. 15 as $l \sim \xi_w \ln L$ and the size of transverse fluctuations is now $l_{\rm tr} \sim l \sim \ln L$. Setting this estimate into Eq. (3.6), we obtain for the scaling relation of the gap

$$\epsilon_1(L) \sim L^{-z}, \qquad (3.8)$$

where z is the dynamical exponent as defined in Eq. (1.1). The distribution of low-energy excitations can be obtained from the observation that an SCD can be localized at any site of the chain, thus $P_L(l) \sim P_L(\ln \epsilon) \sim L$. For a given large L the scaling combination from Eq. (3.8) is $L\epsilon^{1/z}$, thus we have for the gap distribution in the thermodynamic limit

$$P(\epsilon) \sim \epsilon^{-1+1/z}. \qquad (3.9)$$

As already mentioned, z is a continuous function of the quantum control parameter δ and we are going to calculate its exact value in Sec. V.

C. Scaling theory of correlations

The scaling behavior of critical average correlations is also inherently connected to the properties of rare events. Here the quantity of interest is the probability $P^\mu(l)$, which measures the fraction of rare events of the local order parameter m_l^μ. For the surface order parameter m_1^x it is given by the surviving probability, $P^x(1)=P_{\rm surv}$, according to Eq. (3.1). We start with the equal-time correlations in Eq. (2.3). In a given sample there should be local order at both reference points of the correlation function in order to have $C^\mu(r)=O(1)$. This is equivalent of having two SCD's in the sample which occur with a probability of $P_2^\mu(l,l+r)$, which factorizes for large separation $\lim_{r\to\infty} P_2^\mu(l,l+r) = P^\mu(l)P^\mu(L+r)$, since the disorder is uncorrelated. The probability of the occurrence of an SCD at position l, $P^\mu(l)$, has the same scaling behavior as the local order parameter $[m_l^\mu]_{\rm av}=[\langle \phi_\mu | S_l^\mu | 0 \rangle]_{\rm av}$, which behaves at a bulk point, $0<l/L<1$, as

$$[m_l^\mu(L)]_{\rm av} \sim L^{-x^\mu}, \qquad (3.10)$$

whereas for a boundary point, $l=1$, this relation involves the surface scaling dimension x_1^μ. Consequently, $P^\mu(l)$ transforms as $P^\mu(l/b)=b^{-x^\mu}P^\mu(l)$ under a scaling transformation, when lengths are rescaled by a factor $b>1$. As said above, for spatial correlations there should be two independent SCD's we obtain the transformation law

$$[C^\mu(r)]_{\rm av} = b^{-2x^\mu}[C^\mu(r/b)]_{\rm av}. \qquad (3.11)$$

Now taking $b=r$, one recovers the power-law decay in Eq. (2.4) with the exponent

$$\eta^\mu = 2x^\mu. \qquad (3.12)$$

For critical time-dependent correlations the scaling behavior is different from that in Eq. (3.11). This is due to the fact that disorder in the time direction is perfectly correlated and the autocorrelation function in a given sample is $G_l^\mu(\tau)=O(1)$, if there is *one* SCD localized at position l. Therefore the average autocorrelation function $[G_l^\mu(\tau)]_{\rm av}$ scales as the probability of rare events $P^\mu(l)$:

$$[G_l^\mu(\tau)]_{\rm av} = b^{-x^\mu}\tilde{G}_{l/b}^\mu(\ln \tau/b^{1/2}), \qquad (3.13)$$

where we have used the relation in Eq. (3.7), together with $\tau \sim 1/\epsilon_1$ at the critical point, and $\tilde{G}_l^\mu$ is a scaling function, which is expected to be a smooth function of the position l in the bulk of the system. Taking the length scale as $b=(\ln \tau)^2$, we obtain for points l in the volume

$$[G_l^\mu(\tau)]_{\rm av} \sim (\ln \tau)^{-\eta^\mu}, \qquad (3.14)$$

whereas for surface spins, $l=1$, one should use the corresponding surface decay exponent η_1^μ.

Next we turn to study the scaling properties of the average correlation functions in the Griffiths phase, i.e., outside the critical point. For equal-time correlations in a sample $C^\mu(r)=O(1)$, if the SCD extends over a large distance of r, which according to Eq. (3.4) is exponentially improbable. Thus the average spatial correlations decay as

$$[C^\mu(r)]_{\rm av} \sim \exp(-r/\xi), \qquad \xi \sim \xi_w, \qquad (3.15)$$

where ξ_w is defined in Eq. (3.4). On the other hand the autocorrelation function in a sample is $G^\mu(\tau)=O(1)$, if there is one SCD localized at l, which occurs with a probability of $P^\mu(l) \sim 1/L$. Consequently the average autocorrelation function, which scales as $P^\mu(l)$, transforms under a scaling transformation as

$$[G_l^{\mu}(\tau)]_{\rm av} = b^{-1}[G_{l/b}^{\mu}(\tau/b^z)]_{\rm av} \qquad \delta > 0, \qquad (3.16)$$

where we used the scaling combination τ/b^z in accordance with Eq. (1.1). Now taking $b=\tau^{1/z}$ we obtain

$$[G_l^{\mu}(\tau)]_{\rm av} \sim \tau^{-1/z}, \qquad (3.17)$$

for any type of autocorrelations, both in the volume and at the surface.

IV. CRITICAL PROPERTIES

Here we consider in detail the random *XY* and *XX* chains in the vicinity of the critical points, as defined in Eqs. (2.2) and (2.5), respectively. The off-critical properties of the systems in the Griffiths phase are presented afterwards in the following section.

A. Length and time scales

As we argued in the previous section the average behavior of random quantum spin chains are inherently related to the properties of the rare events, which are SCD's, having a coupling distribution of surviving RW character. The typical size of an SCD, as given by ξ_w in Eq. (3.4), is related to the average correlation length of the system, $[\xi]_{\rm av}$. Then using the correspondences in Eqs. (3.1), (3.4), and (3.15), we get the relation

$$[\xi]_{\rm av} \sim |\delta|^{-\nu}, \qquad \nu = 2. \qquad (4.1)$$

The *typical* correlation length $\xi_{\rm typ}$ as measured by the average of the logarithm of the correlation function is different from the *average* correlation length. One can estimate the typical value by studying the formula in Eq. (2.22) for the surface order parameter, where the products are typically of $\Pi_j (J_{2j-1}^y/J_{2j}^x)^2 \sim \exp(\text{const}\cdot|\delta|L)$, thus $[m_s(L,\delta<0)]_{\rm typ} \sim \exp(-\text{const}\cdot|\delta|L) \sim \exp(-L/\xi_{\rm typ})$. Thus we obtain

$$\nu_{\rm typ} = 1. \qquad (4.2)$$

We note that *at the critical point* the largest value of the above products is typically of $\Pi_j (J_{2j-1}^y/J_{2j}^x)^2 \sim \exp(AL^{1/2})$, since the transverse fluctuations in the couplings are of $O(L^{1/2})$; thus we have

$$[m_s(L,\delta=0)]_{\rm typ} \sim \exp(-\text{const}\cdot L^{1/2}).$$

As shown in Eq. (3.6), the value of the smallest gap is related to the size of transverse fluctuations of a SCD, $l_{\rm tr}$. Away from the critical point, where the correlation length is finite, one has $l_{\rm tr} \sim \xi^{1/2}$, and therefore the typical relaxation time of a sample with typical correlation length ξ scales as

$$\ln t_r \sim -\ln \epsilon_i(l) \sim \xi^{1/2}. \qquad (4.3)$$

We note that the results in this part about length and time scales are valid both for the *XY* and *XX* models. They also hold in an identical form for the random TIM,[9,15] which can be understood as a consequence of the mapping of the *XY* chain into decoupled TIM's (see Appendix A). Since the corresponding scaling expressions for the random TIM have been studied in detail in previous numerical work,[13,15] we do not repeat these calculations here.

TABLE I. Decay exponents of critical correlations in the random *XY* and *XX* chains. The exponents with a superscript $^{(*)}$ are those calculated by Fisher with the RG method (Ref. 4), whereas $^{(**)}$ follows from the results of the random TIM in Ref. 9.

	$\eta^x(XY)$	$\eta^x(XX)$	$\eta^z(XY)$	$\eta^z(XX)$
Bulk	$3-\sqrt{5}^{(**)}$	$2^{(*)}$	4	$2^{(*)}$
Surface	1	1	2	1

B. Quasi-long-range order

At the critical point of random quantum chains the equal-time correlations decay with a power law [see Eq. (2.4)], thus there is QLRO in the system. The decay exponent of critical correlations are related to the scaling exponent x^{μ} of the fraction of rare events of the given quantity [see Eq. (3.12)] and its value generally depends on the type of correlations of the disorder; thus it could be different for the *XY* and the *XX* models. Analyzing the scaling properties of the rare events in the *XY* and *XX* chains, we have calculated the critical decay exponents of different correlation functions, both between two spins in the volume and for end-to-end correlations. Our results are presented in Table I. In the following we are going to derive these exponents by analytical and scaling methods and then compare them with the results of numerical calculations.

1. Longitudinal order parameter

We start with the scaling behavior of the longitudinal order parameter m_l^z, which in the *XX* chain is given by the simple formula in Eq. (2.27). Summing over all sites, one gets the sum rule

$$\sum_{l=1}^{L} m_l^z = 1 \ XX \text{ model}, \qquad (4.4)$$

where we have used Eq. (2.15) and the fact that the Φ_q and Ψ_q are normalized. Since this sum rule is valid for the average quantities too, we get immediately

$$[m_l^z]_{\rm av} = L^{-1}\tilde{m}^z(l/L), \qquad (4.5)$$

where $\tilde{m}^z(\tilde{l})$ is a scaling function with $\tilde{l}=l/L$. Consequently for bulk spins the finite-size dependence of the local order parameter is $[m_l^z]_{\rm av} \sim L^{-1}$, thus from Eq. (3.10) we have $x^z(XX)=1$ and from Eq. (3.12) the decay exponent is

$$\eta^z(XX) = 2$$

as given in Table I. A further consequence of the sum rule in Eq. (4.4) is that the average value of the bulk order parameter is the same, if the averaging is performed over any single sample. Thus the order parameter m^z and the correlation function $\langle S_l^z S_{l+r}^z \rangle$ are *self-averaging*. This is quite special in disordered systems where the correlations are generally not self-averaging.[35] The self-averaging properties of the S^z correlations provides an explanation of the accurate numerical determination of the decay exponent $\eta^z(XX)=2$ in previous numerical work.[25,26]

The surface order parameter m_1^z for the *XX* model satisfies the relation $m_1^z = 2(m_1^x)^2$, which follows from Eqs. (2.22)

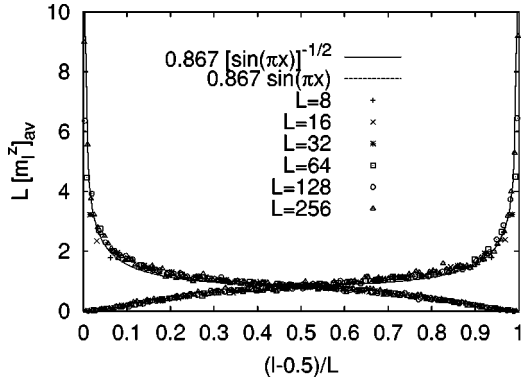

FIG. 2. Finite-size scaling plot of the longitudinal order parameter profiles $[m_l^z]_{\mathrm{av}}$ for the *XX* model at criticality for different system sizes calculated numerically with the fermion method using Eq. (2.27). The data are for the uniform distribution, averaged over 50 000 samples. The conformal results are indicated by full lines.

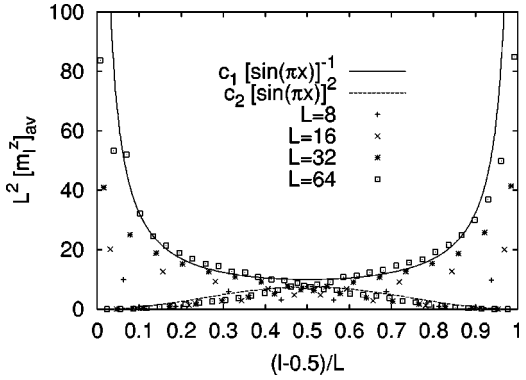

FIG. 3. Finite-size scaling plot of the longitudinal order parameter profiles $[m_l^z]_{\mathrm{av}}$ for the *XY* model at criticality for different system sizes calculated numerically with the fermion method using Eq. (2.27). The data are for the uniform distribution, averaged over 50 000 samples.

and (2.27). Then a rare event with $m_1^x = O(1)$ is also a rare event for the order parameter m_1^z; consequently the fraction of rare events P_1^z is given by the surviving probability in Eq. (3.2). Thus the scaling dimension is $x_1^z = 1/2$ and the decay exponent of critical end-to-end correlations is

$$\eta_1^z(XX) = 1$$

as shown in Table I.

We studied the order parameter profile $[m_l^z]_{\mathrm{av}}$ numerically for large finite systems up to $L = 256$. As shown in Fig. 2 the numerical points of the scaled variable $L[m_l^z]_{\mathrm{av}}$ are on one scaling curve $\tilde{m}^z(\tilde{l})$ for different values of L. The scaling curve has two symmetric branches for odd and even lattice sites, which cross at $l = L/2$. The upper part of the curves in the large L limit is very well described by the function $\tilde{m}^z(\tilde{l})_{\mathrm{u}} = \mathcal{A}\sin(\pi\tilde{l})^{-1/2}$, which corresponds to the conformal result about off-diagonal matrix element profiles:[28]

$$[m_l^\mu]_{\mathrm{av}} \sim \left(\frac{\pi}{L}\right)^{x^\mu} \left(\sin \pi \frac{l}{L}\right)^{x_1^\mu - x^\mu}, \tag{4.6}$$

with $x^z = 1$ and $x_1^z = 1/2$. On the other hand the lower part of the curves in Fig. 2 is given by $\tilde{m}^z(\tilde{l})_{\mathrm{l}} = \mathcal{A}\sin(\pi\tilde{l})$, which corresponds to Eq. (4.6) with $x_2^z = 2$. Thus we obtain that average critical correlations between two spins which are next to the surface are decaying as $[C^z(2,L-1)]_{\mathrm{av}} \sim L^{-4}$. Using the sum rule for the profile in Eq. (4.4) and the conformal predictions, one can determine the prefactor $\mathcal{A}$ from normalization. Then from the equation $\mathcal{A}/2\int_0^1[(\sin \pi x)^{-1/2} + \sin \pi x]dx = 1$, one gets $\mathcal{A} = 0.86735$, which fits well the numerical data on Fig. 2.

These results about the conformal properties of the profile are in agreement with similar studies of the random TIM.[14,15] Thus it seems to be a general trend that critical order parameter profiles of random quantum spin chains are described by the results of conformal invariance, although these systems are strongly anisotropic [see Eq. (4.3)] and therefore not conformally invariant.

Next we turn to study the order parameter m_l^z and the longitudinal correlation function in the random *XY* model. In this model the disorder in the J_l^x and J_l^y couplings is uncorrelated, therefore one can perform averaging in the two subspaces T_σ and T_τ, or in the two decoupled TIM's, independently. Note that the expression for m_l^z in Eq. (2.26) is given as a product of two vector components, where each vector belongs to different subspaces and have the same average behavior. Since the couplings entering the two separate eigenvalue problems are independent, one gets for the disorder average

$$[m_l^z]_{\mathrm{av}} = [\Phi_1(l)]_{\mathrm{av}} \cdot [\Psi_2(l)]_{\mathrm{av}}. \tag{4.7}$$

Since the probability for m_l^z being of order 1 is the product of the probabilities for $\Phi_1(l)$ and $\Psi_2(l)$ being of order 1, we conclude that the scaling dimension for m_l^z in the random *XY* chain is twice that for the random *XX* chain. Thus the decay exponents are

$$\eta^z(XY) = 4$$

and

$$\eta_1^z(XY) = 2$$

in the bulk and at the surface, respectively, as shown in Table I.

The numerical results about the order parameter profile is shown in Fig. 3. The data collapse is satisfactory, although not as good as for the *XX* model. Similar conclusion holds for the relation with the conformally predicted profile, which is also presented in Fig. 3.

2. Transverse order parameter

We start with the surface order parameter m_1^x as given by the simple formula in Eq. (2.22). This formula is identical both for the *XY* and *XX* models and its average behavior follows from the adsorbing random-walk mapping in Sec. III A. Then from Eqs. (3.1) and (3.2) one gets $x_1^x = 1/2$ and

$$\eta_1^x = 1,$$

both for the random *XY* and *XX* models, as shown in Table I. The value of the decay exponents follows also from the mapping to two TIM's. As shown in Eq. (A8) in Appendix A, the

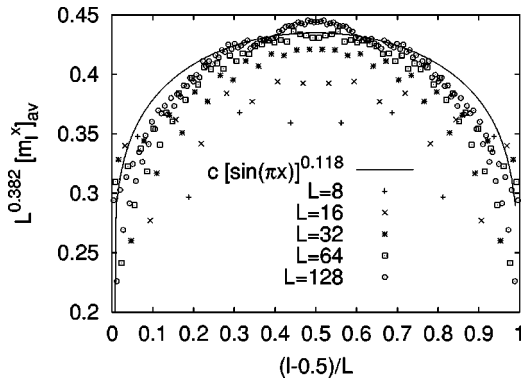

FIG. 4. Transverse order parameter profile $[m_l^x]_{\rm av}$ for the *XY* model at criticality for different system sizes calculated numerically with the fermion method using Eq. (2.23). The data are for the uniform distribution, averaged over 50 000 samples.

correlation function $\langle S_{2l}^x S_{2l+2r}^x \rangle$ is expressed as the product of spin correlations in the two TIM's, one with open boundary conditions, but the other taken with fixed-spin boundary conditions in terms of dual variables. For end-to-end correlations this second factor in the product is unity, since it is the correlation between two fixed spins. Therefore end-to-end correlations between the random TIM and the random *XY* and *XX* models are identical and the decay exponent corresponds to the value in Table I.

For bulk correlations one can easily find the answer for the *XY* model with the mapping in Eq. (A8). When the two points of reference are located far from the boundary, the boundary condition does not matter and after performing the independent averaging for the two factors of the product one obtains $[\langle S_{2l}^x S_{2l+2r}^x \rangle]_{\rm av} = 1/4[\langle \sigma_l^x \sigma_{l+r}^x \rangle]_{\rm av}^2$; thus

$$\eta^x(XY) = 2\,\eta(\mathrm{TIM}) = 3 - \sqrt{5}, \tag{4.8}$$

where the last result follows from Fisher's RG calculation.[9] (As shown in Ref. 36 the rare events for the bulk order parameter in the TIM are samples having a coupling distribution of average persistence character.) The scaling exponent $x^x(XY)$ can identically be obtained from the expression of the order parameter profile in Eq. (2.23), which is in the form of a product of the two Ising order parameters and for the *XY* model the two factors are averaged independently.

For the *XY* model the numerically calculated profile is shown in Fig. 4. The scaling plot with the exponents in Table I is reasonable, although larger systems and even more samples would be needed to reach the expected asymptotic behavior, as predicted by conformal invariance in Eq. (4.6).

The arguments leading to the prediction (4.8) for the transverse bulk order parameter exponent do not apply for the *XX* model and one cannot obtain a simple estimate for the bulk decay exponent from Eqs. (A8) or (2.23) due to the following reason. The expressions with the parameters of the two quantum Ising chains contain real and dual variables for the two (σ and τ) systems. Since $J_l^x = J_l^y = J_l$ a domain of strong couplings in the σ chain corresponds to a domain of weak couplings in the τ chain and vice versa. Therefore the rare events of the TIM can not be simply related to the rare-events of the *XX* chain.

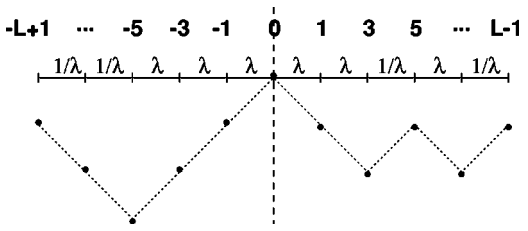

FIG. 5. Sketch of a bond configuration for a chain of length $2L-1$ that gives a nonvanishing transverse magnetization $m^x \sim \mathcal{O}(1)$ for the central (bulk) spin. The example is for the extreme binary distribution. Weak couplings ($J_{2i-1} = \lambda$) correspond to downward steps of the random walk on both sides of the central spin (here at 0). Note that both the right and the left halves of the random walk have surviving character, i.e., do not cross the starting point.

The value for $\eta^x(XX)$, however, can be obtained by the following argument. For simplicity let us consider the extreme binary distribution in which $J_{2i} = 1$ and $J_{2i-1} = \lambda$ or $1/\lambda$ with probability 1/2, taking the limit $\lambda \to 0$. Then, from Eq. (2.22), one gets only then a nonvanishing transversal surface magnetization, when the disorder configuration has a surviving walk character (meaning $\Pi_{i=1}^{l} J_{2i-1} < \infty$ for all $l = 1, \ldots, L/2-1$). This implies also for general distributions of couplings that $m_1^x \sim \mathcal{O}(1)$ only if the surface spin is *weakly* coupled to the rest of the system. It is instructive to note the difference to the surface magnetization in the TIM, where $m_1^x \sim \mathcal{O}(1)$ when the surface spin is *strongly* coupled to the rest of the system, meaning that $\Pi_{i=1}^{l} (1/J_i) < \infty$ for all $l = 1, \ldots, L-1$ for the extreme binary distribution.

The same remains true for a bulk spin, which also has nonvanishing transverse magnetization only if it is weakly coupled to the rest of the system (the trivial example being the case where both its couplings to the left and to the right are exactly zero, which gives the maximum value $m_1^x = 1/2$). Thus the central spin in a chain of length, say $2L-1$, has $m^x \sim \mathcal{O}(1)$ if and only if the bond configurations on both sides have surviving character, as it is depicted in Fig. 5 for the extreme binary distribution. Since the probability $P_{\rm surv}(L/2)$ for a configuration of $L/2$ couplings to represent a surviving walk is $P_{\rm surv}(L/2) \sim L^{-1/2}$, it is

$$m_l^x \sim \{P_{\rm surv}(L/2)\}^2 \sim L^{-1}, \quad \text{i.e., } x^x(XX) = 1. \tag{4.9}$$

From this one obtains

$$\eta^x(XX) = 2, \tag{4.10}$$

as given in Table I.

We verified the strong correlation between weak coupling and nonvanishing transverse order parameter numerically in the following way: We considered a chain with $L+1$ sites and the couplings at both sides of the central spin were taken randomly from a distribution called *SW*,[37] which represents those samples in the uniform distribution which has a surface magnetization of $m_1^x(SW) > 1/4$. (Thus cutting one of the couplings to the central spin results in a local magnetization greater than 0.25.) Then we calculated numerically the order parameter at the central spin and its average value over the *SW* configurations $[m_{L/2}^x]_{\rm sw}$ as given in Table II. As seen in the table the averaged surface order parameter stays constant

TABLE II. Surface and bulk transverse order parameters averaged over 50 000 SW configurations for the uniform distribution.

L	$2[m_1^x]_{sw}$	$2[m_{L/2}^x]_{sw}$
16	0.817	0.531
32	0.806	0.471
64	0.799	0.431
128	0.792	0.413
256	0.791	0.383

for large values of L, whereas the bulk order parameter decreases very slowly, actually slower than any power. The data can be fitted by $[m_{L/2}^x]_{sw} \sim (\ln L)^{-\sigma}$, with $\sigma \approx 0.5$. Thus we conclude that the numerical results confirm Eq. (4.10), although there are strong logarithmic corrections, which imply for the average transverse correlations

$$[C^x(r)]_{av} \sim r^{-2} \ln^{-1}(r) \qquad XX \quad \text{model.} \qquad (4.11)$$

These strong logarithmic corrections render the numerical calculation of critical exponents very difficult.[26,25] In earlier numerical work using smaller finite systems, disorder dependent exponents were reported.[25] We believe that these numerical results can be interpreted as effective, size-dependent exponents and the asymptotic critical behavior is indeed described by Eq. (4.11).

Note that our results in Table I satisfy the relation $\eta^x(XX) = \eta^z(XX)$, both in the volume and at the surface, which corresponds to Fisher's RG result.[4] In this way we have presented independent justification of Fisher's RS phase picture, where the average correlations are dominated by random singlets, so that the distance between the pairs could be arbitrarily large.

We checked numerically the above theoretical predictions in the random XX model. In Fig. 6 we present the scaled m_l^x profiles for the binary distribution for finite systems up to $L = 512$. The profiles have a broad plateau and the points of $L^{x^x} m_l^x$ do not perfectly fall on one scaling curve due to strong finite-size effects. Even system sizes as large as $L = 512$ appear to be insufficient to get rid of such correction terms. Therefore we have calculated the effective size-dependent $x^x(L)$ exponents by two-point fitting. For this we

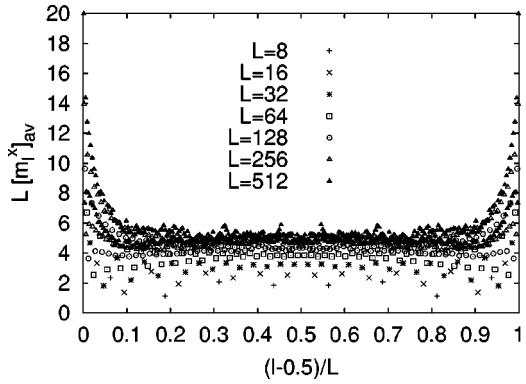

FIG. 6. Transverse order parameter profile $[m_l^x]_{av}$ for the XX model at criticality for different system sizes calculated numerically with the fermion method using Eq. (2.23). The data are for the binary distribution, averaged over 50 000 samples.

TABLE III. Effective bulk scaling dimension of the transverse order parameter in the random XX chain.

L	$x^x(L)$
16	0.635
32	0.677
64	0.730
128	0.823
256	0.872
512	0.910

have averaged the order parameter in the middle of the profile for $L/4 < l < 3L/4$ and compared this average value for finite systems with $L/2$ and L sites. As seen in Table III the effective exponents are monotonously increasing with the size of the system and they are not going to saturate,[38] even for $L = 512$.

From the data in Table III one cannot make an accurate estimate of the limiting value of $x^x(L)$, but it is clear that $x^x(L)$ grows at least up to the theoretical limit $x^x = 1$, although it could, in principle, reach even a larger value. We note that similar observation was made by Henelius and Girvin from the average S^x correlation function, where the effective η^x exponents seem to grow over the theoretically predicted value of $\eta^x = 2$ (see Fig. 2 of Ref. 26).

C. Autocorrelations

According to the scaling theory in Sec. III C the decay of average critical autocorrelations in random quantum spin chains is ultraslow; it takes place in logarithmic time scales, as given in Eq. (3.14). Here we confirm these predictions with the results of numerical calculations. We start with the surface autocorrelation function $[G_1^x(\tau)]_{av}$ for the XX model, which is calculated in the binary distribution ($\lambda = 4$) on finite systems up to $L = 128$. As seen in Fig. 7 (top) the logarithmic time dependence is well satisfied and the decay exponent is found in agreement with $\eta_1^x(XX) = 1$ as given by the scaling result in Eq. (3.14). For bulk spin critical autocorrelations we considered $[G_{L/2}^z(\tau)]_{av}$ for the XX model. Again the numerical results in Fig. 7 (bottom) are consistent with a logarithmic decay with an exponent $\eta^z(XX) = 2$, as given in Table I.

Next we turn to study the *distribution* of critical autocorrelations. As we have seen, the average behavior is logarithmically slow, but for typical samples, as described in Appendix B, one expects a faster decay with a power-law time dependence. Then $G_l^\mu(\tau) \sim \tau^{-\gamma}$ and the γ exponent could vary from sample to sample. Such type of ''multiscaling'' behavior of the autocorrelations has been recently observed by Kisker and Young[39] in the random quantum Ising model. In Fig. 8 we have numerically checked this assumption for the critical autocorrelations $G_1^x(\tau)$ and $G_{L/2}^z(\tau)$, respectively, of the random XX chain, the average behavior of which have been studied before. As seen in Fig. 8 we have obtained indeed a good data collapse of the probability distributions $P^\mu(\gamma)$ in terms of the scaling variable $\gamma = -\ln G_l^\mu / \ln \tau$ for both types of autocorrelations, but the scaling curve in the two cases are different.

The average correlation functions generally have contributions from the scaling function $P^\mu(\gamma)$, but there could be

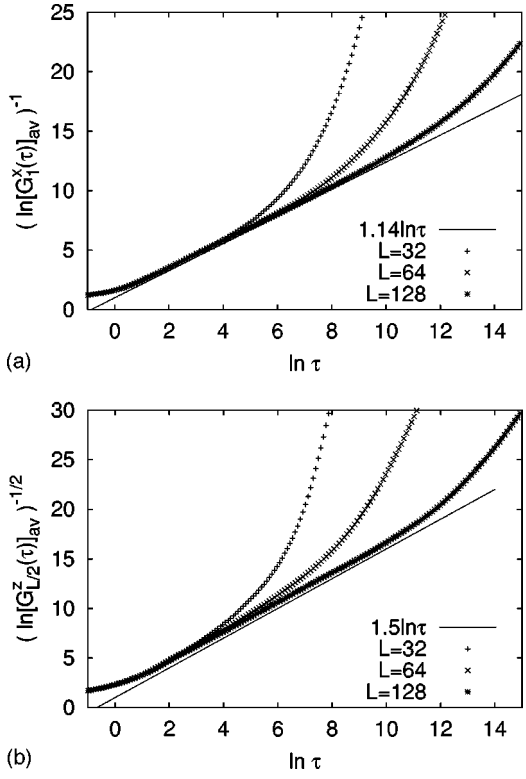

FIG. 7. Spin autocorrelation function $[G_l^{\mu}(\tau)]_{\rm av}$ for the XX model for $L=32$, 64, and 128 calculated numerically with the fermion method using Eqs. (2.28) and (2.33). The data are for the binary distribution ($\lambda=4$), averaged over 50 000 samples. (a) (top) shows $l=1$, the surface transverse autocorrelations, (b) (bottom) shows $l=L/2$, the bulk longitudinal autocorrelations.

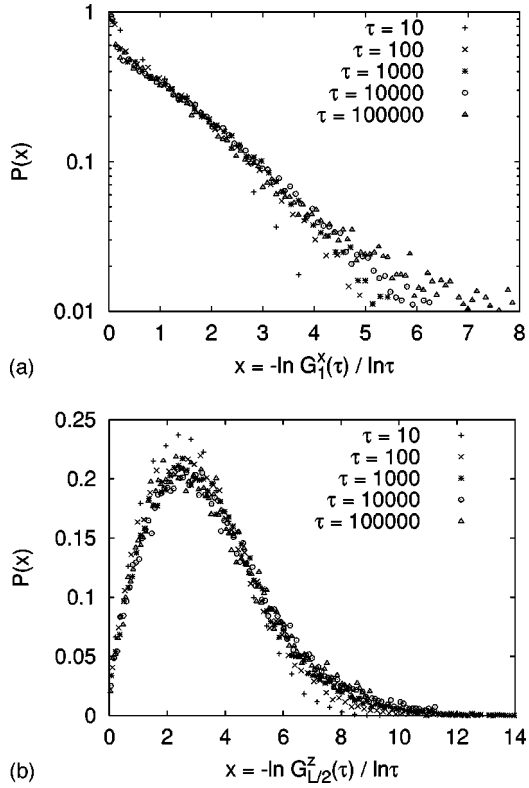

FIG. 8. Scaling plot of the probability distribution of the autocorrelation function $G_l^{\mu}(\tau)$ for the XX model for different values of τ at criticality ($L=128$). The data are for the uniform distribution averaged over 100 000 samples. (a) (top) shows $l=1$, the surface transverse autocorrelations, (b) (bottom) shows $l=L/2$, the bulk longitudinal autocorrelations.

also nonscaling contributions, as found for the random quantum Ising chain in Ref. 40. The scaling contribution is coming from the small γ part of the scaling function, which, according to Fig. 8 (top) for the autocorrelations $G_1^x(\tau)$, approaches a finite value linearly, $P^x(\gamma)\sim A+B\,\gamma$. Thus we have for the average autocorrelations

$$[G_1^x(\tau)]_{\rm av}=\int_0^{\infty}P^x(\gamma)G_1^x(\tau)d\gamma$$

$$\sim\int_0^{\infty}(A+B\gamma)\exp(-\gamma\ln\tau)d\gamma$$

$$\sim A(\ln\tau)^{-1}+B(\ln\tau)^{-2}, \qquad (4.12)$$

in agreement with the scaling result in Eq. (3.14) and with the numerical result in Fig. 8 (top). We note that the correction to scaling contribution to the average autocorrelations in Eq. (4.12) is also logarithmic.

For the critical autocorrelation $G_{L/2}^z(\tau)$ the scaling function in Fig. 8 (bottom) for small γ approaches zero linearly;[41] $P^z(\gamma)\sim\gamma$. Thus the scaling contribution to the average autocorrelation, as evaluated along the lines of Eq. (4.12), is $[G_1^x(\tau)]_{\rm av}\sim(\ln\tau)^{-2}$, in agreement with the scaling result in Eq. (3.14).

V. GRIFFITHS PHASE

Random quantum systems exhibit unusual off-critical properties: they are gapless in an extended region, $0<|\delta|<\delta_G$, as a result of the so-called Griffiths-McCoy singularities.[19,42] In this Griffiths phase the system is critical in the time direction, although spatial correlations decay exponentially.

Quantitatively the basic information is contained in the distribution of low energy excitations $P(\epsilon)$ as given in Eq. (3.9). With this the average autocorrelations can be obtained as

$$[G(\tau)]_{\rm av}\sim\int_0^{\infty}P(\epsilon)\exp(-\tau\epsilon)d\epsilon\sim\tau^{-1/z}, \qquad (5.1)$$

which is expected to hold for any component of the spin.[43] In this way we have recovered the scaling result in Eq. (3.17). In the Griffiths phase also some thermodynamic quantities are singular, which are expressed as an integral of the autocorrelation function. We mention the local susceptibility χ_l^x at site l, which is defined through the local order parameter m_l^x in Eq. (2.18) as

$$\chi_l^x=\lim_{H_l^x\to 0}\frac{\partial m_l^x}{\partial H_l^x}, \qquad (5.2)$$

where H_l^x is the strength of the local longitudinal field, which enters the Hamiltonian in Eq. (2.1) via an additional term $H_l^xS_l^x$. χ_l^x can be expressed as

$$\chi_l^x = 2\sum_{\langle n|} \frac{|\langle n|S_l^x|0\rangle|^2}{E_n - E_0}; \tag{5.3}$$

thus its average value scales in finite systems as $\chi_l^x(L) \sim L^{z-1}$, where we have used the scaling relation in Eq. (3.8) and the fact that the matrix element in Eq. (5.3) is $\sim 1/L$, since an SCD can be localized at any site of the chain. For a small finite temperature T we can use the scaling relations $T \sim \epsilon \sim L^{-z}$ and we have for the singular behavior

$$[\chi_l^x(T)]_{\rm av} \sim T^{-1+1/z}. \tag{5.4}$$

To estimate the temperature dependence of the average specific heat $[C(T)]_{\rm av}$, we calculate first the average excitation energy per SCD with $P(\epsilon)$ in Eq. (3.9) as $\int \epsilon P(\epsilon) d\epsilon \sim \epsilon^{1/z+1}$, which is proportional to the thermal excess energy per spin $\sim T^{1/z+1}$, from which we obtain

$$[C(T)]_{\rm av} \sim T^{1/z}. \tag{5.5}$$

We note that several other physical quantities are singular in the Griffiths phase (nonlinear susceptibility, higher excitations, etc.) and the corresponding singularities are expected to be related to the dynamical exponent z. For a detailed study of this subject in the random quantum Ising model, see Ref. 22.

In the following we calculate the exact value of the dynamical exponent using the same strategy as for the random quantum Ising model in Refs. 20 and 21. Our basic observation is the fact that the eigenvalue problem of the T_σ (or T_τ) matrix can be mapped through a unitary transformation to a Fokker-Planck operator, which appears in the master equation of a Sinai diffusion, i.e., random walk in a random environment.[23] The transition probabilities of the latter problem are then expressed with the coupling constants of the spin model. The Griffiths phase of the spin model corresponds to the anomalous diffusion region of the Sinai walk and from the exact results about the scaling form of the energy scales in this problem one obtains for the dynamical exponent of the XY model

$$\left[\left(\frac{J^x}{J^y}\right)^{1/z}\right]_{\rm av} = 1, \tag{5.6}$$

whereas for the XX model the result follows with the correspondences in Eq. (2.8). For the binary distribution in Eq. (2.6) the Griffiths phase extends over the region $1 < J_0^y < \lambda$ and z is given by

$$(J_0^y)^{1/z} = \cosh\left(\frac{\ln \lambda}{z}\right). \tag{5.7}$$

For the uniform distribution

$$z \ln(1 - z^{-2}) = -\ln J_0^y, \tag{5.8}$$

and the Griffiths phase extends to $1 < J_0^y < \infty$.

Next we are going to study numerically the Griffiths phase and to verify some of the scaling results described above. In this respect we shall not consider those quantities which have an equivalent counterpart in the random quantum Ising model (distribution of energy gaps, local susceptibility, specific heat, etc.), since that model has already been thoroughly investigated numerically.[13,16,15,22] The autocorrelation functions, however, are different in the two models and we are going to study those in the following.

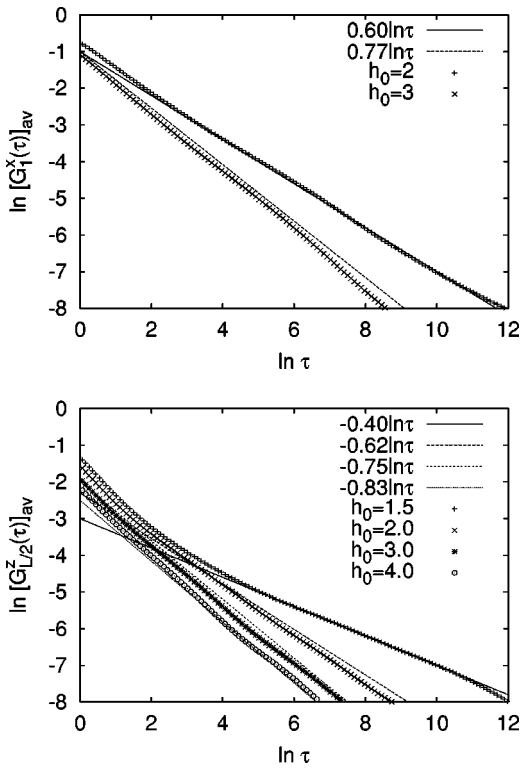

FIG. 9. The average surface (top) and bulk (bottom) autocorrelation function $[G^{\mu}_{L/2;1}(\tau)]_{\rm av}$ of the XX model in the Griffiths phase for various values of h_0. The straight lines have a slope of $1/z(h_0)$, where the dynamical exponent $z(h_0)$ agrees well with the exact value determined via the formula (5.6). The data are for the uniform distribution averaged over 50 000 samples of size $L = 128$.

The average bulk longitudinal autocorrelation function $[G^z_{L/2}(\tau)]_{\rm av}$ of the XX model is shown in Fig. 9 in a log-log plot at different points of the Griffiths phase. The asymptotic behavior in Eq. (5.1) is well satisfied and the dynamical exponents obtained from the slope of the curves are in good agreement with the analytical results in Eq. (5.6). A similar conclusion can be drawn from the average surface transverse autocorrelations $[G^x_1(\tau)]_{\rm av}$, as shown in Fig. 9.

Next we study the distribution of the autocorrelation functions. In Fig. 10 the distribution of the bulk longitudinal autocorrelation function of the XX model is given at different times τ. As argued in Appendix B, the typical autocorrelations are of a stretched exponential form

$$G(\tau) \sim \exp(-\text{const}\, \tau^{1/(1+z)}), \tag{5.9}$$

thus the relevant scaling variable is

$$\alpha = -\frac{\ln G(\tau)}{\tau^{1/(z+1)}}. \tag{5.10}$$

Using this scaling argument, we obtained a good data collapse of the points of the distribution function as shown in Fig. 10. We note that for the random quantum Ising model Young[16] has also derived the scaling function from phenomenological arguments,

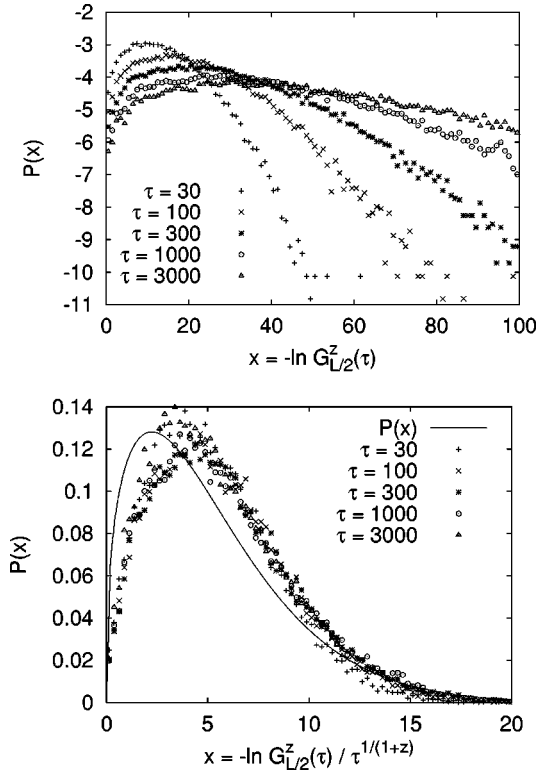

FIG. 10. (Top): Probability distribution of the bulk longitudinal autocorrelation function of the *XX* model in the Griffiths phase for $h_0=1.5$. The data are for the uniform distribution from 100 000 samples of size $L=128$. (Bottom): Scaling plot of the data in the top figure. The scaling variable $[\ln G(\tau)]/\tau^{1/(z+1)}$ contains the dynamical exponent $z(h_0)$ known from the formula (5.6). The full curve is the theoretical prediction in Eq. (5.11) using the exact value of $z(h_0=1.5)=2.659$ and a fit parameter $c=0.22$.

$$P(x)=c(cx)^{1/z}\exp\left(-\frac{z}{1+z}(cx)^{1+1/z}\right), \qquad (5.11)$$

which is also presented in Fig. 10. One can see considerable differences between the numerical and theoretical curves. Similar tendencies have been noticed for the random quantum Ising model in Ref. 16. The discrepancies are probably due to strong correction to scaling or finite-size effects. These corrections, however, do not affect the scaling form in Eq. (5.10).

VI. DISCUSSION

In this section we first discuss the possible extension of our results to random *XXZ* chains and to higher dimensional systems, and then we conclude with a brief summary of our findings.

A. Random *XXZ* chains

The more general *XXZ* (or *XYZ*) Heisenberg spin chain, where the Hamiltonian in Eq. (2.1) contains an additional interaction term of the form

$$H_Z=\sum_{l=1}^{L-1} J_l^z S_l^z S_{l+1}^z \qquad (6.1)$$

can be treated perturbatively when $J_l^z \ll J^x, J^y$. Here we consider the *XXZ* chain, with $J_l^z=\varepsilon J_l$ and $\varepsilon \ll 1$. To see the scaling behavior of the energy gap we express the small perturbation H_Z in terms of two decoupled TIM's (see Appendix A) as

$$H_Z=-\frac{1}{4}\sum_{i=1}^{L/2-1}(J_{2i-1}^z\sigma_i^z\tau_i^z+J_{2i}^z\sigma_i^x\sigma_{i+1}^x\tau_i^x\tau_{i+1}^x), \qquad (6.2)$$

whose expectation value in the unperturbed ground state is just the product of the local energy densities of the TIM's. The perturbative correction to the gap, $\Delta_z(L)=\langle 1|H_z|1\rangle - \langle 0|H_z|0\rangle$, evaluated with the states of the unperturbed Hamiltonian, $\langle 0|$ and $\langle 1|$, is proportional to the gap of one of the random TIM's, $\epsilon_\sigma(L)$. At the critical point[15] $\epsilon_\sigma(L) \sim \exp(-\text{const}\cdot L^{1/2})$, which is the same scaling form as for the *XY* model in Eq. (3.7). Thus the scaling relation in Eq. (4.3) is valid also for the *XXZ* chain. In the Griffiths phase one has again $\epsilon_\sigma(L)\sim L^{-z}$, and the dynamical exponent *z*, has the same value as in Eq. (5.6). Thus we arrive at the conclusion that also in the Griffiths phase the corresponding scaling relation in Eq. (1.1) is valid in the same form for the random *XXZ* chain, at least for small J^z couplings.

Next we study the asymptotic properties of average critical correlations in the random *XXZ* model through the scaling behavior of the local order parameters. As we argued in Sec. III, these quantities are related to the fraction of rare events, P^μ, and here we are going to investigate the influence of the perturbation H_Z to P^μ. We start with the surface transverse order parameter m_1^x and recall that it is maximal, i.e., $m_1^x=1/2$, if the surface spin is disconnected in the *XY* plane, i.e., $J_1^x=J_1^y=0$. Evidently the value of $m_1^x=1/2$ does not change for any finite value of the coupling J_1^z. Now consider the infinite-randomness fixed point of the *XX* chain with the extreme binary distribution, where a rare event is represented by couplings with a surviving random-walk configuration and with $m_1^x=O(1)$. Roughly speaking, a rare event is formally equivalent to a situation in which there is a very weak surface coupling of $J_1=O(L^{-1/2})$, where *L* is the system size. Then switching on homogeneous and finite couplings J^z the lowest excitation of the chain stays localized at the surface, since the shape of the wave function does not change significantly in first-order perturbation theory. Consequently the surface order parameter is still $m_1^x=O(1)$, and the sample is a rare event for the *XXZ* chain, too. For small random couplings J_l^z the accumulated fluctuations in J_l^z are divergent as $\sim L^{1/2}$; however, these are still negligible compared with the fluctuations in the transverse couplings. Thus the rare events of the *XX* chain are identical with those appearing in the *XXZ* chain for small values of the random longitudinal couplings. As a consequence the critical end-to-end average correlations decay with the same exponent as given in Table I. Since the rare events for other local order parameters are also connected to SCD's with localized wave functions the stability of the infinite-randomness fixed point holds for the other critical correlations, too. Actually, it seems to be plausible that the attracting region of the *XX* fixed point extends up to $[\ln J^x]_{\text{av}}>[\ln J^z]_{\text{av}}$, i.e., where the

average transverse couplings are larger than the longitudinal ones, thus up to the random XXX fixed point, in agreement with Fisher's conjecture.[4]

B. Higher dimensions

In one dimension the topology is special since there is only a single path between two points, whereas in higher dimensional lattices one has several distinct paths connecting two points. This topological difference is essential when random XX magnets are considered in higher dimensions. Let us consider again the surface transverse order parameter and construct a rare event in the extreme binary distribution. For this purpose the surface spin should be extremely weakly coupled to the bulk of the system. Thus considering any non-self-crossing path from the spin to the volume, one should have a surviving random-walk configuration in the couplings. In higher dimensions the number of such paths grows exponentially with the size of the system L, thus the fraction of rare events, which is related to the length as a power in one dimension, becomes exponentially small in higher dimensions. Consequently the infinite-randomness fixed point picture is not applicable here and one concludes that the critical properties of higher dimensional XX and Heisenberg antiferromagnets are controlled by conventional random fixed points. This result is also in agreement with numerical RG calculations in two dimensions.[12] We note that in contrast to random Heisenberg antiferromagnets the random ferromagnetic quantum Ising models in higher dimensions are still controlled by infinite-randomness fixed points.[45,12]

VII. SUMMARY

Quantum spin chains in the presence of quenched disorder show unusual critical properties, which are controlled by the infinite-randomness fixed point. A common feature of these systems is that various physical properties, especially those related to local order parameters and correlation functions are not self-averaging and their average behavior is determined by the rare events (or rare regions), which give the dominant contribution, although their fraction is vanishing in the thermodynamic limit. In this paper we have performed a detailed study of the scaling behavior of rare events appearing in the random XY and XX chains. We identified the rare events as strongly coupled domains, where the coupling distribution follows some surviving random walk character. From the scaling properties of the rare events we have identified the complete set of critical decay exponents and found exact results about the correlation length exponent and the scaling anisotropy. Here we note that most (not all) of the random walk arguments are for the extreme binary distribution, but all analytical predictions from these arguments are supported by numerical data for generic distributions. Thus we expect the results to be generally valid and universality should hold because of the infinite-randomness fixed point governing the critical behavior of these systems. In this respect the extreme binary distribution represents one possible explicit construction of the infinite-randomness fixed point.

Another aspect of our work was the study of dynamical correlations. We have obtained the asymptotic behavior of the average autocorrelation function and determined the scaling form of the distribution of autocorrelations. In the off-critical regime we investigated the singular physical quantities in the Griffiths phase. In particular we have obtained exact expression for the dynamical exponent z, which is a continuous function of the quantum control parameter and the singularities of all physical quantities can be related to its value.

ACKNOWLEDGMENTS

This work was partially performed during our visits in Köln and Budapest, respectively. F.I.'s work was supported by the Hungarian National Research Fund under Grant No. OTKA TO23642, TO25139, MO28418, and by the Ministery of Education under Grant No. FKFP 0596/1999. H.R. was supported by the Deutsche Forschungsgemeinschaft (DFG). We thank L. Turban for helpful comments on the manuscript.

APPENDIX A: MAPPING TO DECOUPLED ISING QUANTUM CHAINS

We start here with the observation in Sec. II B that the eigenvalue matrix T in Eq. (2.14) can be represented as a direct product $T=T_\sigma\otimes T_\tau$. The tridiagonal matrices T_σ, T_τ of size $L\times L$ represent transfer matrices of directed walks, which are in one-to-one correspondence with Ising chains in transverse field[30] defined by the Hamiltonians

$$H_\sigma=-\frac{1}{4}\sum_{i=1}^{L/2-1} J_{2i}^x\sigma_i^x\sigma_{i+1}^x-\frac{1}{4}\sum_{i}^{L/2} J_{2i-1}^y\sigma_i^z,$$
$$H_\tau=-\frac{1}{4}\sum_{i=1}^{L/2-1} J_{2i}^y\tau_i^x\tau_{i+1}^x-\frac{1}{4}\sum_{i}^{L/2} J_{2i-1}^x\tau_i^z. \tag{A1}$$

Here the $\sigma_i^{x,z}$ and $\tau_i^{x,z}$ are two sets of Pauli matrices at site i and there are free boundary conditions for both chains. We can then write $H_{XY}=H_\sigma+H_\tau$. Note the symmetry $\sigma_i^{x,z}\leftrightarrow\tau_i^{x,z}$ and $J_l^x\leftrightarrow J_l^y$, thus anisotropy in the XY model has different effects in the two Ising chains.

One can easily find the transformational relations between the XY and Ising variables:

$$\sigma_i^x=\prod_{j=1}^{2i-1}(2S_j^x),\quad \sigma_i^z=4S_{2i-1}^yS_{2i}^y,$$
$$\tau_i^x=\prod_{j=1}^{2i-1}(2S_j^y),\quad \tau_i^z=4S_{2i-1}^xS_{2i}^x, \tag{A2}$$

whereas the inverse relations are the following:

$$2S_{2i-1}^x=\sigma_i^x\prod_{j=1}^{i-1}\tau_j^z,\quad 2S_{2i}^x=\sigma_i^x\prod_{j=1}^{i}\tau_j^z,$$
$$2S_{2i-1}^y=\tau_i^x\prod_{j=1}^{i-1}\sigma_j^z,\quad 2S_{2i}^y=\tau_i^x\prod_{j=1}^{i}\sigma_j^z. \tag{A3}$$

We note that a relation between the XY model and two decoupled Ising quantum chains in the thermodynamic limit has been known for some time;[44,4] here we have extended

this relation for finite chains with the appropriate boundary conditions. These are essential in mapping local order parameters and end-to-end correlation functions.

End-to-end correlations are related as

$$\langle S_1^x S_L^x \rangle = \frac{1}{4} \langle \sigma_1^x \sigma_{L/2}^x \rangle \left\langle \prod_{i=1}^{L/2} \tau_i^z \right\rangle = \frac{1}{4} \langle \sigma_1^x \sigma_{L/2}^x \rangle, \quad \text{(A4)}$$

since in the ground state $\langle \Pi_{i=1}^{L/2} \tau_i^z \rangle = 1$. Similarly,

$$\langle S_1^y S_L^y \rangle = \tfrac{1}{4} \langle \tau_1^x \tau_{L/2}^x \rangle, \quad \text{(A5)}$$

thus the end-to-end correlations in the two models are in identical form. As a consequence the corresponding decay exponent in the random models, η_1^x in Table I is the same in the two systems and the same conclusion holds also for the correlation length exponent, ν in Eq. (4.1). These results are also independent of the type of correlation of the disorder, and thus are valid both for the *XY* and *XX* models.

Correlations between two spins at general positions $2l$ and $2l+2r$ are related as

$$\langle S_{2l}^x S_{2l+2r}^x \rangle = \frac{1}{4} \langle \sigma_l^x \sigma_{l+r}^x \rangle \left\langle \prod_{i=1}^{r} \tau_{l+i}^z \right\rangle. \quad \text{(A6)}$$

The second factor in the right-hand side, $\langle \Pi_{i=1}^{r} \tau_{l+i}^z \rangle$, defines a stringlike order parameter[26] which can be expressed in a simpler form in terms of the dual Ising variables $\tilde{\tau}_{i+1/2}^x$, which are defined on the bonds of the original Ising chain as

$$\tilde{\tau}_{i+1/2}^z = \tau_i^x \tau_{i+1}^x,$$

$$\tau_i^z = \tilde{\tau}_{i-1/2}^x \tilde{\tau}_{i+1/2}^x. \quad \text{(A7)}$$

Under the duality transformation fields and couplings are exchanged; therefore the vanishing bonds at the two ends of an open chain are transformed to vanishing fields; thus the dual chain has two end spins fixed to the same state. So we obtain for the correlations in Eq. (A6)

$$\langle S_{2l}^x S_{2l+2r}^x \rangle = \tfrac{1}{4} \langle \sigma_l^x \sigma_{l+r}^x \rangle \langle \tilde{\tau}_{l+1/2}^x \tilde{\tau}_{l+r+1/2}^x \rangle^{++}, \quad \text{(A8)}$$

where the superscript $^{++}$ denotes fixed-spin boundary condition. For nonsurface points the average value of the correlation function in Eq. (A8) depends on the type of disorder correlations. For the *XY* model, where the disorder is uncorrelated, the two factors in Eq. (A8) can be averaged separately, whereas this is not possible for the *XX* model. We treated this point in Sec. IV B 2.

APPENDIX B: DISTRIBUTION OF AUTOCORRELATION FUNCTIONS

The autocorrelation functions are represented by the general form

$$G(\tau) = \sum_k |M_k|^2 \exp(-\tau \Delta E_k), \quad \text{(B1)}$$

where the dominant contributions to the sum in Eq. (B1) are from SCD's, which are localized at some distance l from the spin and have a very small excitation energy $\Delta E(l)$. The scaling form of $\Delta E(l)$ follows from the considerations in Sec. III B and one obtains from Eqs. (3.7) and (3.8)

$$\Delta E(l) \sim \begin{cases} \epsilon_0 \exp(-A l^{1/2}), & \delta = 0 \\ \epsilon_0 l^{-z(\delta)}, & \delta < 0 \end{cases} \quad \text{(B2)}$$

at the critical point and in the Griffiths phase, respectively, where ϵ_0 denotes the energy scale. Thus the larger the distance from the spin the larger the probability to have an SCD with a very small energy. For the matrix element $|M(l)|^2$ the tendency is the opposite, since the overlap with the wave function of the SCD is (exponentially) decreasing with the distance. The corresponding scaling form can be read from the typical behavior of the surface order parameter as given below and above Eq. (4.2) as

$$|M(l)|^2 \sim \begin{cases} \exp(-B l^{1/2}), & \delta = 0 \\ \exp(-l/\xi_{\text{typ}}), & \delta < 0. \end{cases} \quad \text{(B3)}$$

Then $G(\tau)$ in Eq. (B1) can be approximated by a sum which runs over SCD's localized at different distances l and this sum is dominated by the largest term with $l = l_0$:

$$G(\tau) \sim |M(l_0)|^2 \exp[-\tau \Delta E(l_0)]. \quad \text{(B4)}$$

Using the scaling forms in Eqs. (B2) and (B3) one gets the following result.

At the critical point the characteristic distance is $l_0 = [\ln(\tau \epsilon_0 A/B)/A]^2$ and the typical autocorrelation function decays as a power:

$$G(\tau) \sim \tau^{-B/A}, \qquad \delta = 0. \quad \text{(B5)}$$

Thus the relevant scaling variable of the problem is

$$\gamma = -\frac{\ln G(\tau)}{\ln \tau}, \qquad \delta = 0. \quad \text{(B6)}$$

In the Griffiths phase the characteristic distance has a power-law τ dependence, $l_0 = \xi_{\text{typ}} (\tau \epsilon_0 z)^{1/(z+1)}$, which is, however, different from the average scaling form in Eq. (1.1). The typical autocorrelations now are in a stretched exponential form:

$$G(\tau) \sim \exp\left[-(\tau \epsilon_0 z)^{1/(z+1)} \left(1 + \frac{1}{z} \right) \right], \quad \delta \neq 0, \quad \text{(B7)}$$

and the relevant scaling variable is given in Eq. (5.10).

[1] F.D.M. Haldane, Phys. Lett. **93A**, 464 (1983).
[2] See H. Rieger and A. P Young, in *Complex Behavior of Glassy Systems*, edited by M. Rubi and C. Perez-Vicente, Lecture Notes in Physics Vol. 492 (Springer-Verlag, Heidelberg, 1997), p. 256 for a review on the Ising quantum spin glass in a transverse field.
[3] C. Dasgupta and S.K. Ma, Phys. Rev. B **22**, 1305 (1979).
[4] D.S. Fisher, Phys. Rev. B **50**, 3799 (1995).
[5] R.A. Hyman, K. Yang, R.N. Bhatt, and S.M. Girvin, Phys. Rev. Lett. **76**, 839 (1996); Kun Yang and R.N. Bhatt, *ibid.* **80**, 4562 (1998).
[6] M. Fabrizio and R. Mélin, Phys. Rev. Lett. **78**, 3382 (1997).
[7] C. Monthus, O. Golinelli, and Th. Jolicoeur, Phys. Rev. Lett. **79**, 3254 (1997).
[8] K. Hida, Phys. Rev. Lett. **83**, 3297 (1999).
[9] D.S. Fisher, Phys. Rev. Lett. **69**, 534 (1992); Phys. Rev. B **51**, 6411 (1995).
[10] E. Westerberg, A. Furusaki, M. Sigrist, and P.A. Lee, Phys. Rev. B **55**, 12 578 (1997).
[11] T. Hikihara, A. Furusaki, and M. Sigrist, cond-mat/9905352 (unpublished).
[12] O. Motrunich, S.-C. Mau, D.A. Huse, and D.S. Fisher, Phys. Rev. B **61**, 1160 (2000).
[13] A.P. Young and H. Rieger, Phys. Rev. B **53**, 8486 (1996).
[14] F. Iglói and H. Rieger, Phys. Rev. Lett. **78**, 2473 (1997).
[15] F. Iglói and H. Rieger, Phys. Rev. B **57**, 11 404 (1998).
[16] A.P. Young, Phys. Rev. B **56**, 11 691 (1997).
[17] R.H. McKenzie, Phys. Rev. Lett. **77**, 4804 (1996).
[18] H. Rieger and F. Iglói, Europhys. Lett. **39**, 135 (1997).
[19] R.B. Griffiths, Phys. Rev. Lett. **23**, 17 (1969).
[20] F. Iglói and H. Rieger, Phys. Rev. E **58**, 4238 (1998).
[21] F. Iglói, L. Turban, and H. Rieger, Phys. Rev. E **59**, 1465 (1999).
[22] F. Iglói, R. Juhász, and H. Rieger, Phys. Rev. B **59**, 11 308 (1999).
[23] See J.P. Bouchaud and A. Georges, Phys. Rep. **195**, 127 (1990) for a review on diffusion in random environment.
[24] S. Haas, J. Riera, and E. Dagotto, Phys. Rev. B **48**, 13 174 (1993).
[25] H. Röder, J. Stolze, R.N. Silver, and G. Müller, J. Appl. Phys. **79**, 4632 (1996).
[26] P. Henelius and S.M. Girvin, Phys. Rev. B **57**, 11 457 (1998).
[27] H. Rieger, R. Juhász, and F. Iglói, Eur. Phys. J. B **13**, 409 (2000).
[28] L. Turban and F. Iglói, J. Phys. A **30**, L105 (1997).
[29] E. Lieb, T. Schultz, and D. Mattis, Ann. Phys. (N.Y.) **16**, 407 (1961).
[30] F. Iglói and L. Turban, Phys. Rev. Lett. **77**, 1206 (1996).
[31] J. Stolze, A. Nöppert, and G. Müller, Phys. Rev. B **52**, 4319 (1995).
[32] D.S. Fisher, Physica A **263**, 222 (1999).
[33] The extreme binary distribution represents one possible explicit construction of the infinite-randomness fixed point.
[34] F. Iglói, L. Turban, D. Karevski, and F. Szalma, Phys. Rev. B **56**, 11 031 (1997).
[35] B. Derrida, Phys. Rep. **103**, 29 (1984).
[36] H. Rieger and F. Iglói, Europhys. Lett. **45**, 673 (1999).
[37] In the binary distribution SW denotes the set of coupling distributions with a *surviving walk* character.
[38] It is not feasible to increase the size of the system further, primary not due to computational demand, but due to inaccuracies in the numerical routines, even in 64-bit precision. The origin of this numerical difficulty are those samples with an extremely small excitation energy.
[39] J. Kisker and A.P. Young, Phys. Rev. B **58**, 14 397 (1998).
[40] D.S. Fisher and A.P. Young, Phys. Rev. B **58**, 9131 (1998).
[41] For a finite system the scaling function approaches a finite limiting value of $P^z(\gamma=0,L)\sim L^{-1/2}$, which is checked numerically.
[42] B. McCoy, Phys. Rev. Lett. **23**, 383 (1969).
[43] For correlations of such spin components which exhibit long-range order one considers the connected autocorrelation function and in Eq. (3.9) the distribution is related to the second gap.
[44] I. Peschel and K.D. Schotte, Z. Phys. B: Condens. Matter **54**, 305 (1984).
[45] C. Pich, A.P. Young, H. Rieger, and N. Kawashima, Phys. Rev. Lett. **81**, 5916 (1998); H. Rieger and N. Kawashima, Eur. Phys. J. B **9**, 233 (1999); T. Ikegami, S. Miyashita, and H. Rieger, J. Phys. Soc. Jpn. **67**, 2761 (1998).